ELSEVIER

Catalysis Today 56 (2000) 371–378

CATALYSIS TODAY

www.elsevier.com/locate/cattod

Characterisation by EPR spectroscopy

E. Abi Aad (F-5) *, A. Aboukaïs (F-5)

Laboratoire de Catalyse et Environnement, E.A. 2598, Université du Littoral-Côted'Opale, MREID,
145, Avenue Maurice Schumann, 59140 Dunkerque, France

Contributors: E. Abi Aad, D. Courcot, A. Aboukaïs (F-5); A. Brückner, M. Baerns (D-1); M. Guelton (F-6); J.C. Vedrine (F-1)

Abstract

The fresh and used EUROCAT II V_2O_5–WO_3/TiO_2 catalysts have been studied by electron paramagnetic resonance. For both samples, V^{4+} in clusterlike arrangement and two sites corresponding to VO^{2+} ions in octahedral symmetry axially distorted were found. It has been shown that the TiO_2 phase transformation (anatase → rutile) occurs at lower temperature (1073 K) for the EUROCAT II catalysts than the WO_3/TiO_2 support. Impurities of Fe^{3+} ions were detected both on the catalysts and on the WO_3/TiO_2 support. Q-band measurements have allowed a difference in the environment of the Fe^{3+} ions caused by the SCR process to be observed. Finally, traces of Ti^{3+} ions in the anatase phase have been detected. ©2000 Elsevier Science B.V. All rights reserved.

Keywords: Electron paramagnetic resonance; Catalytic reduction; EUROCAT oxide

1. Introduction

Vanadia/titania (V_2O_5/TiO_2) binary systems have been widely investigated by the electron paramagnetic resonance (EPR) technique [1–4]. In fact, EPR is a highly sensitive technique which allows investigation of paramagnetic species having one or more unpaired electron either in the bulk or at the surface of various solids. The information gained using EPR may provide a detailed description both of the nature of the species (e.g., V^{4+} or VO^{2+}) and their co-ordination symmetries in the solid. Depending on the synthesis process of the solid, the vanadium content and the thermal treatment, different V(IV) species could be detected by EPR. For instance, V(IV) clusters give rise to a broad signal owing to significant dipolar interactions, whereas isolated V(IV) species exhibit hyperfine structure deriving from the interaction of free electrons ($3d^1$) with the magnetic nuclear moment of ^{51}V ($I = 7/2$). In this case the EPR signal splits into eightfold lines of all anisotropic components. From the spin-Hamiltonian parameters, the Zeeman effect and the isotropic and anisotropic exchange interactions, EPR spectra can be interpreted.

V_2O_5/TiO_2 based catalysts are known to be active in the selective catalytic reduction (SCR) of nitrogen oxides [5–7]. Chen and Yang have studied the effect of tungsten oxide on the V_2O_5/TiO_2 catalysts for the SCR of nitric oxide with ammonia [8]. This addition of WO_3 grants the V_2O_5–WO_3/TiO_2 system more stability and increases its activity in the SCR reaction. In a recent work, Paganini et al. [9] have studied a V_2O_5–WO_3/TiO_2 catalyst and observed that the V(IV) species of the ternary systems are remarkably different from that of V_2O_5/TiO_2 systems.

In this work, we report a characterisation by EPR of the nature of vanadium (IV) species in

---

* Corresponding author. Tel.: +33-3-2865-8268;
fax: +33-3-2865-8239.

PII: S0920-5861(99)00297-7

V_2O_5–WO_3/TiO_2 EUROCAT II catalysts and their interactions. We identify some paramagnetic species present as impurities either in the support or in the catalysts.

2. Experimental

2.1. EPR measurements

EPR spectra were recorded at 293 and 77 K with a Bruker EMX spectrometer using the X-band and the Q-band microwave frequencies, a power supply sufficiently small (7–13 mW) to avoid saturation effects and a modulation frequency of 100 kHz. Modulation amplitudes from 1 to 10 G were used. The g-values were determined by measuring the magnetic field, H, and the microwave frequency. All the thermal and vacuum treatments of the samples were carried out in a microflow reactor, which is assembled with a quartz EPR tube to allow the introduction of the solid into the resonance cavity without exposure to air.

Simulation of the EPR spectra of ions with $S > \frac{1}{2}$ and $I \neq 0$ was done by diagonalization of the spin-Hamiltonian:

$$H = g\beta\vec{\mathrm{H}}\vec{\mathrm{S}} + A\vec{\mathrm{S}}\vec{\mathrm{I}} + D[S_z^2 - \tfrac{1}{3}S(S+1)] + E(S_x^2 - S_y^2)$$

where D and E are the crystal-field parameters, $\vec{\mathrm{S}}$ and $\vec{\mathrm{I}}$ the corresponding vectors of electronic and nuclear spin, g is the g-factor tensor and A the hyperfine structure tensor. In the case of $S = \frac{1}{2}$, $D = E = 0$.

2.2. Samples

The EPR measurements were performed for two samples of V_2O_5–WO_3/TiO_2: fresh and used in the SCR process. The WO_3/TiO_2 support which was obtained from the industrial partner and used for the preparation of these catalysts was also analysed. All samples were crushed in an agate mortar and then introduced into an EPR tube for analysis. In some cases, measurements were made after calcination at 673–1073 K for 4 h in a flow of dry air or after outgassing the samples under vacuum at 573 K and 7.5×10^{-6} mbar for 30 min.

3. Results and discussions

Fig. 1 shows the X-band EPR spectra recorded at 77 K for the fresh and used samples before any treatment and after outgassing. The EPR spectra of both untreated catalysts are the superimposition of different signals in the range of $g = 2$ mainly caused by V(IV) species and a signal at $g = 4.26$ which is due to isolated Fe^{3+} impurity ions in rhombic symmetry $E/D = \frac{1}{3}$. There are almost no differences in the spectra of the fresh and used catalyst indicating that the local structure of the paramagnetic species is not greatly influenced by the SCR process. Nevertheless, the intensities calculated by double integration of the spectra show that the fresh sample presents more paramagnetic species than the used one.

After outgassing the samples, their colours change from yellow–green to grey. In both cases, a better resolution of the EPR spectra is observed (Fig. 1). Moreover, the V(IV) signals intensity increases indicating higher amount of these species. This may be the result of the reducing outgassed conditions. Indeed, in the same time the intensity of the signal corresponding to Fe^{3+} decreases (Fig. 1).

The most obvious difference between the spectra of the fresh and the used catalyst is revealed by a signal at $g = 2.23$ which appears in the fresh catalyst but not in the used one (Fig. 2). This signal is only observed at room temperature and disappears at 77 K indicating that it is caused by species which are coupled by antiferromagnetic exchange interactions [10]. Moreover, this signal at $g = 2.23$ was not always observed in the fresh catalyst even for spectra recorded at room temperature. After calcination of a fresh sample under a flow of dry air at 673 K, the intensity of this signal drastically decreases and becomes nil for a calcination temperature of 1073 K indicating that the signal at $g = 2.23$ may be due to an ageing effect explaining by the way its aleatoric appearance. There are different possibilities for the assignment of this signal; it could be due to an antiferromagnetic Fe^{3+} oxide phase. From iron-containing zeolites it is well known that oxidic iron clusters give rise to signals in the range of $g \approx 2.2$–2.3 [10]. On the other hand, the signal could arise from antiferromagnetically interacting V^{4+}–V^{4+} or V^{4+}–W^{5+} ion pairs with a total spin of $S = 1$. For a reliable attribution of this signal, more investigations should be done by computer simulation.

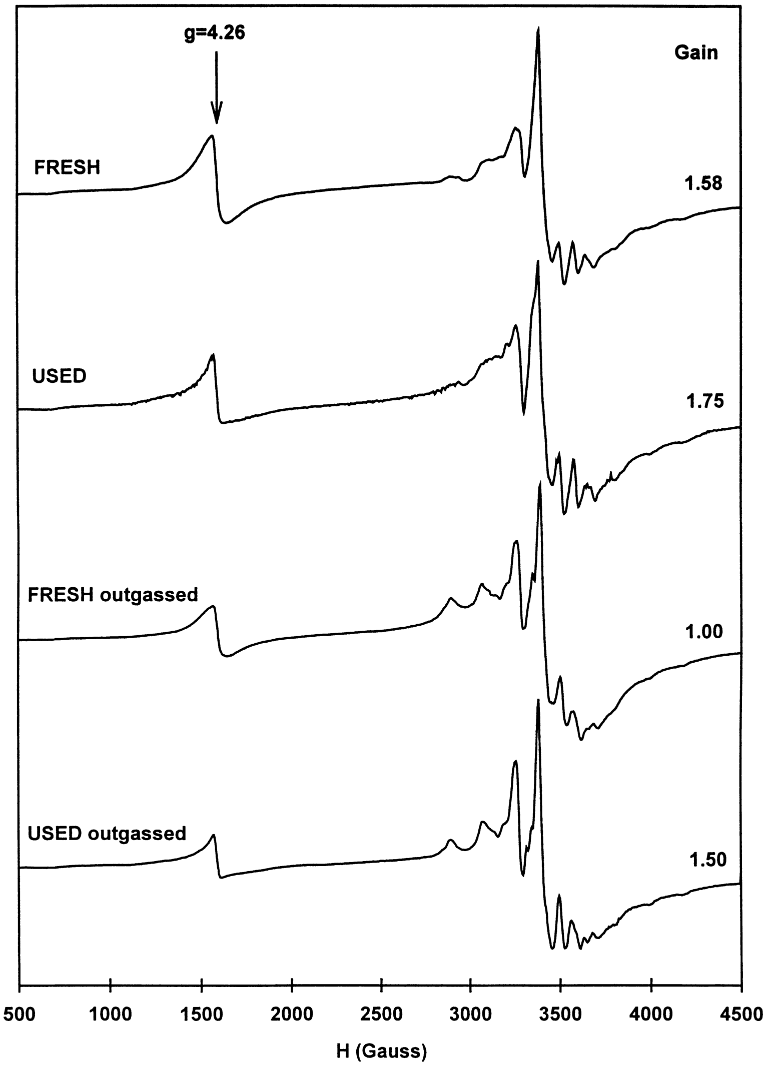

Fig. 1. X-band EPR spectra recorded at 77 K for the untreated and outgassed samples.

Furthermore, a study of the signal intensity variation versus the recording temperature would be of major interest.

In addition to signals relating to Fe^{3+} and V(IV) species, when the fresh catalyst is calcined at 1073 K (Fig. 2), a hyperfine structure of six lines centred at $g_{iso} = 2.009$ appears. The EPR parameters of this signal ($g_{iso} = 2.009$; $A_{iso} = 94.6$ G) are similar to those already obtained for Mn^{2+} ions located in sites with distorted octahedral symmetry in different matrices [11–13]. Unlike iron, which was detected by other analysis methods, manganese impurities in the EUROCAT II fresh sample have only been detected by EPR.

Owing to the complexity of the EPR spectra obtained for the used and fresh samples (Figs. 1 and 2), especially signals observed in the range of $g = 2$, EPR measurements were performed on the WO_3/TiO_2 support before the addition of the vanadium to permit precise attribution of the signals due to V(IV) species. Thus, Fig. 3 illustrates the EPR spectra obtained for the WO_3/TiO_2 support calcined at different temperatures. For all spectra, one can observe the signal at $g = 4.26$ which was attributed to isolated Fe^{3+} ions in

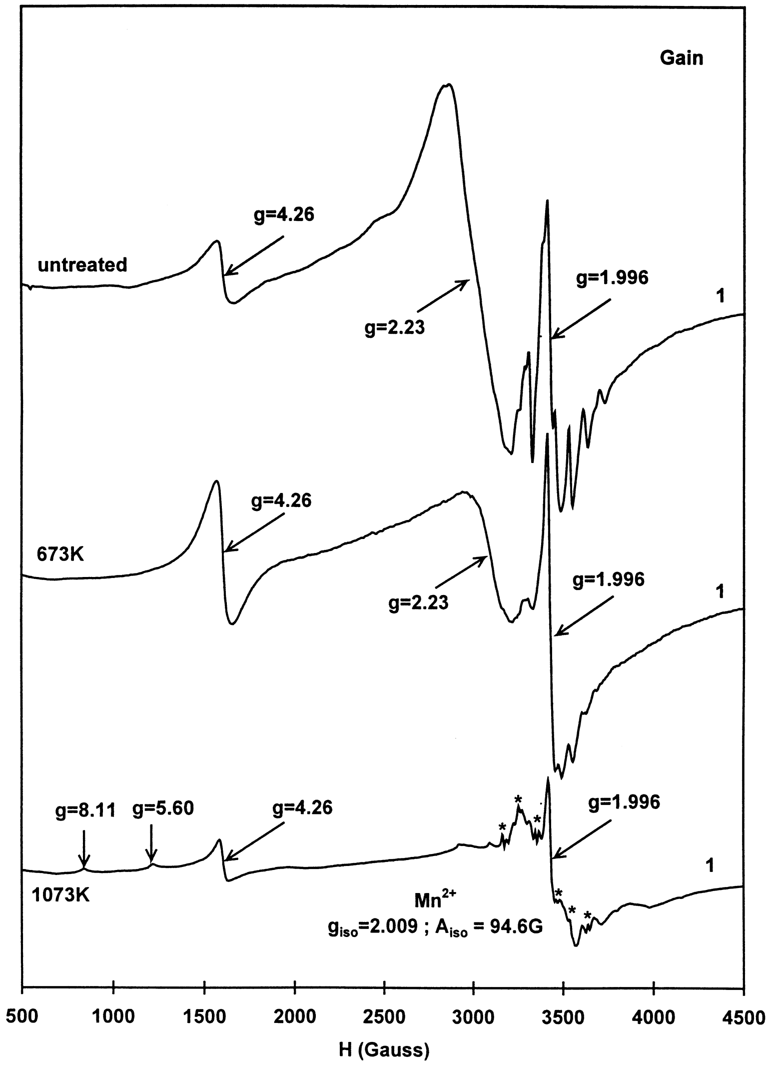

Fig. 2. X-band EPR spectra recorded at 298 K for the fresh catalyst untreated and calcined at 673–1073 K.

rhombic symmetry. Moreover, substitutionally incorporated Fe^{3+} ions are present in the TiO_2 matrix since resonance at $g=2$ is observed [14]. In addition, the intensity of this signal ($g=1.996$) increases for a calcination temperature of 1073 K (Fig. 3) indicating that more Fe^{3+} ions are incorporated in the matrix which is a known feature at high temperature [15].

By subtracting the EPR spectra obtained for the WO_3/TiO_2 support from those obtained in V_2O_5–WO_3/TiO_2 samples (under the same calcination conditions), higher precision can be obtained for the deduced EPR parameters. Two different isolated V(IV) sites have been identified. However, the spectral parameters of these two sites are rather similar (Table 1). The observation of a broad V^{4+} signal in the range of $g=2$, is due to strong dipolar interactions between the paramagnetic ions and reveals the presence of vanadyl agglomerates in the solid (Fig. 1, Table 1). Furthermore, the reproduction of the experimental spectra by computer simulation confirmed the presence of the different V(IV) sites.

In the case of isolated V (IV) species, information about their environment can be obtained from g and A values. For all samples $g_{\mathrm{iso}}=1.960$–1.963

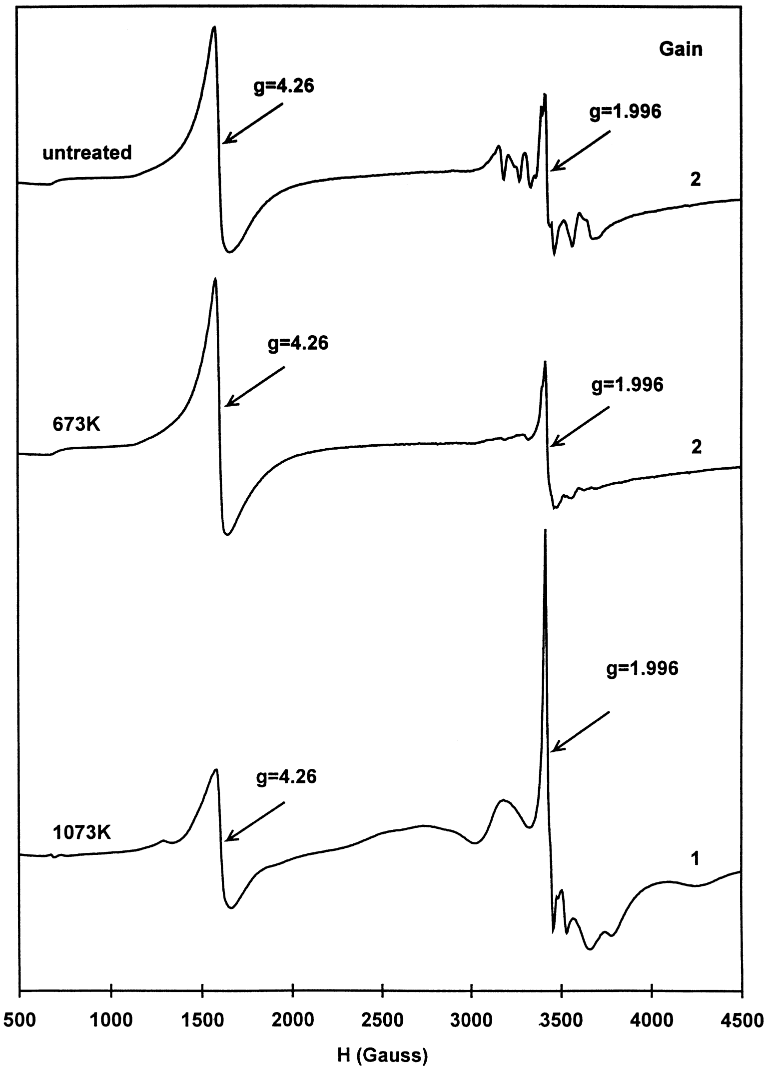

Fig. 3. X-band EPR spectra recorded at 77 K for the WO_3/TiO_2 support untreated and calcined at 673–1073 K.

Table 1
EPR parameters obtained for the V(IV) species at 77 K on the fresh and used samples

Sample	$g_{//}$	$g_{\perp}$	$A_{//}$ (G)	$A_{\perp}$ (G)	g_{iso}	A_{iso} (G)
Fresh	1.923	1.983	185.6	78	1.963	113.8
Fresh	1.908	1.986	182.8	78.6	1.960	113.3
Fresh	1.917	1.984	–	–	1.962	–
Used	1.917	1.985	179	80.4	1.962	113.3
Used	1.911	1.988	188.6	77.2	1.962	114.4
Used	1.919	1.985	–	–	1.963	–

and $A_{\mathrm{iso}} = 113.3$–114.4 G. These could correspond to VO^{2+} ions in octahedral symmetry axially distorted since $1.955 < g_{\mathrm{iso}} < 1.980$ and $80\,\mathrm{G} < A_{\mathrm{iso}} < 120\,\mathrm{G}$ [1]. Generally, lower g_{iso} and A_{iso} values are expected in the cases of V^{4+} species in octahedral symmetry $1.920 < g_{\mathrm{iso}} < 1.950$ and $60\,\mathrm{G} < A_{\mathrm{iso}} < 90\,\mathrm{G}$ [3,16–18].

More information can be gained by comparing the Fe^{3+} lines observed at low magnetic field ($g > 4$) for the WO_3/TiO_2 support and the fresh catalyst when both have been calcined at 1073 K (Fig. 4). Iron, which

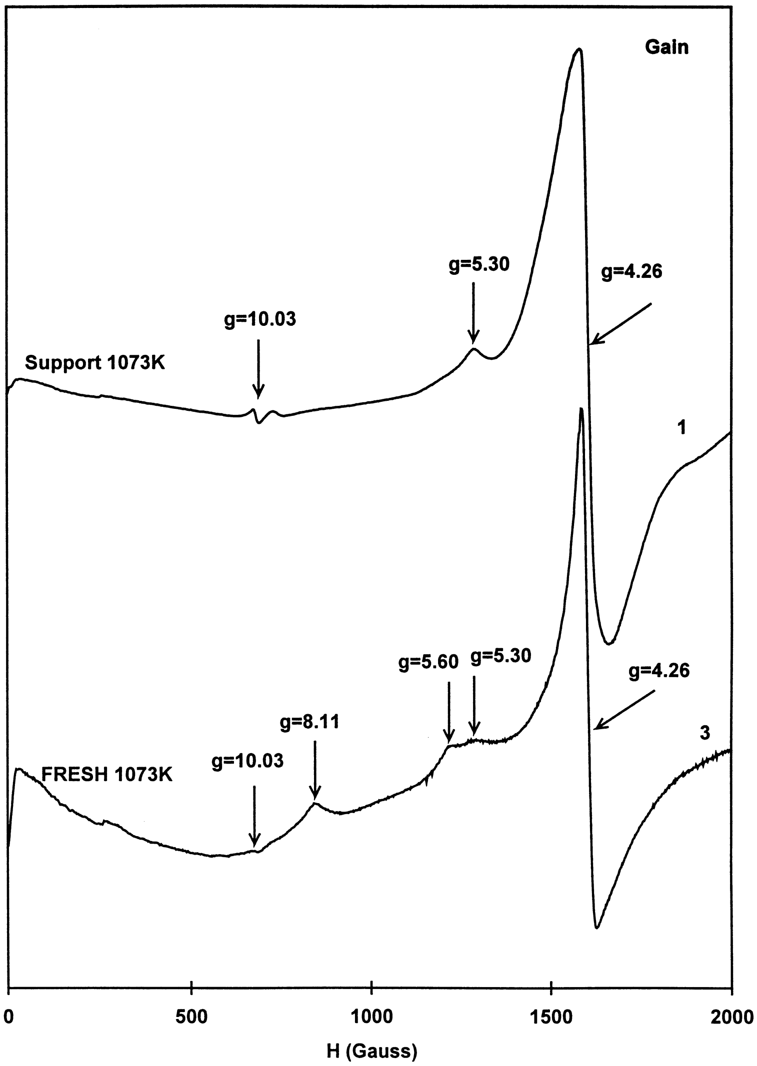

Fig. 4. Fe^{3+} lines of the EPR spectra recorded at 77 K for the WO_3/TiO_2 support and the fresh catalyst both calcined at 1073 K.

is present in the WO_3/TiO_2 support before the addition of vanadium, is in a very similar environment in the fresh and used catalysts and the WO_3/TiO_2 support when these solids are untreated or calcined at low temperatures (<1073 K) (Figs. 1 and 3). However, after the calcination of the catalysts and the support at 1073 K, the EPR spectra show important differences in the Fe^{3+} ions environment (Fig. 4). Indeed, the width of the line at $g = 4.26$ decreases from $\Delta H = 84$ G for the WO_3/TiO_2 support to $\Delta H = 40$ G for the fresh catalyst. Two lines at $g = 5.60$ and $g = 8.11$, characteristic of Fe^{3+} ions in TiO_2 rutile phase [15], are observed for the catalyst but not for the WO_3/TiO_2 support. These observations clearly indicate that the TiO_2 phase transformation (anatase → rutile) occurs at lower temperature for the fresh catalyst than the WO_3/TiO_2 support exempt from vanadium. Similar results are obtained for the used catalyst.

Q-band EPR measurements were performed on the fresh and used V_2O_5–WO_3/TiO_2 catalysts. Fig. 5 shows the Q-band EPR spectra recorded at room temperature for these two samples. As in the case of X-band, the Q-band EPR parameters of the V(IV) species for the fresh and used catalyst are very sim-

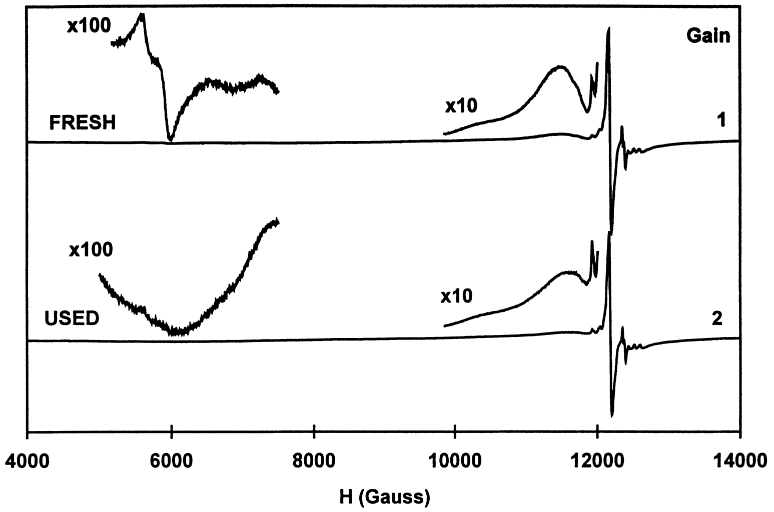

Fig. 5. Q-band EPR spectra recorded at 298 K for the untreated fresh and used catalysts.

ilar, but signal intensities are different. In fact, the Q-band measurements confirm that after the SCR process, the EPR signal intensity decreases. Furthermore, the signal at $g \approx 4.26$ attributed to Fe^{3+} ions is not observed on the Q-band spectrum of the used sample (Fig. 5). It seems that the environment of the Fe^{3+} species changes after using the catalyst in the SCR process. This phenomenon was not shown by the X-band measurements. In addition to signals described above, a broad signal superposed on the lines corresponding to the V^{4+} hyperfine structure is observed. This signal is centred at $g = 2.051$ and can be better observed using Q-band EPR. The width of this signal is $\Delta H_{pp} = 760$ G for the fresh sample and $\Delta H_{pp} = 510$ G for the used sample (Fig. 5). By comparison with data reported in the literature, this signal could be assigned to Fe^{3+} ions with high dipolar interactions [14,15]. Such a signal could arise from Fe^{3+} ions closely neighboured or oxidic Fe (III) clusters.

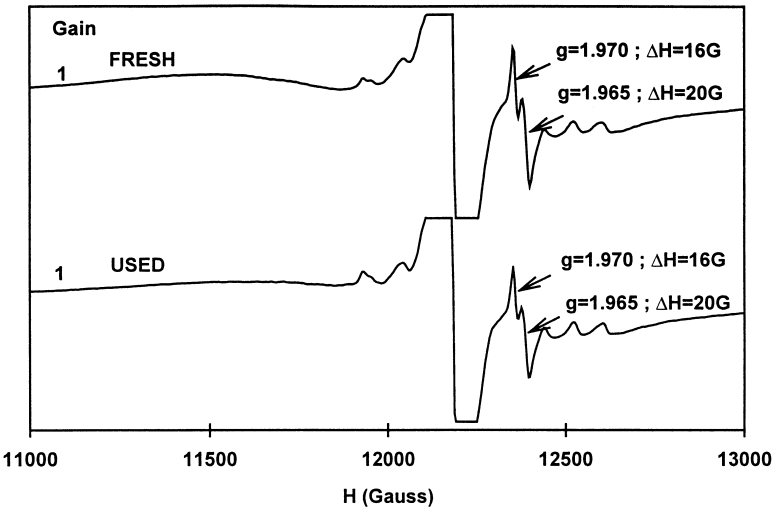

Fig. 6. Ti^{3+} lines of the Q-band EPR spectra recorded at 298 K for the untreated fresh and used catalysts.

In addition to the signals observed above, two narrow lines at $g=1.965$ and 1.970 are detected by Q-band measurements (Figs. 5 and 6) and are characteristic of Ti^{3+} ions in the anatase phase [19–20]. This result agrees with those obtained by electrical conductivity measurements (see for instance the work of Herrmann et al. on these samples, published in this issue). Finally, no traces of isolated W^{5+} ions (d^1) were detected in the fresh, used or WO_3/TiO_2 support of the EUROCAT II samples neither in X-band nor Q-band. Indeed, such species (W^{5+}) in TiO_2 matrix exhibit an EPR signal at high magnetic field with: $g_x=1.472$, $g_y=1.443$ and $g_z=1.594$ [21].

4. Conclusion

EPR characterisation does not reveal significant differences between the fresh and used EUROCAT II catalysts. For both samples, V^{4+} in clusterlike arrangement and two sites corresponding to VO^{2+} ions in octahedral symmetry axially distorted are found. The EPR measurements performed on the WO_3/TiO_2 support show the same Fe^{3+} ions present as impurities in the catalysts. Thorough study of this signal at different temperatures shows that the TiO_2 phase transformation (anatase → rutile) occurs at lower temperature (1073 K) for the EUROCAT II catalysts than the WO_3/TiO_2 support. The Q-band EPR analysis has shown changes in the environment of the Fe^{3+} ions caused by the SCR process. Finally, traces of Ti^{3+} ions in the anatase phase have been detected.

Acknowledgements

The *“Laboratoire de Catalyse et Environnement (F-5)”* would like to thank the Conseil Général du Nord, the Région Nord — Pas de Calais and the European Community for financial support in the EPR apparatus purchase.

References

[1] H. Takahashi, M. Shiotani, H. Kobayashi, J. Sohma, J. Catal. 14 (1969) 134.
[2] P. Meriaudeau, J.C. Vedrine, Nouv. J. Chim. 2 (1978) 133.
[3] G. Centi, S. Perathoner, F. Trifiro, A. Aboukaïs, C.F. Aïssi, M. Guelton, J. Phys. Chem. 96 (1992) 2617.
[4] A. Aboukaïs, C.F. Aïssi, M. Dourdin, D. Courcot, M. Guelton, E.M. Serwicka, E. Giamello, F. Geobaldo, A. Zecchina, A. Foucault, J.C. Vedrine, Catal. Today 20 (1994) 87.
[5] H. Bosch, F. Janssen, Catal. Today 2 (1988) 369.
[6] N.-Y. Topsøe, H. Topsøe, J.A. Dumesic, J. Catal. 151 (1995) 226.
[7] N.Y. Topsøe, J.A. Dumesic, H. Topsøe, J. Catal. 151 (1995) 241.
[8] J.P. Chen, R.T. Yang, Appl. Catal. A: General 80 (1992) 135.
[9] M.C. Paganini, L. Dall’Acqua, E. Giamello, L. Lietti, P. Forzatti, G. Busca, J. Catal. 166 (1997) 195.
[10] D. Goldfarb, M. Bernardo, K.G. Strohmaier, D.E.W. Vaughan, H. Thomann, J. Am. Chem. Soc. 116 (1994) 6344.
[11] F.W. Breivagel, V. Sarkissian, J. Chem. Phys. 48 (1968) 2442.
[12] O.J. Rubio, P. Munoz, O.J. Boldu, Y. Chen, M.M. Abraham, J. Chem. Phys. 70 (1979) 633.
[13] E. Abi Aad, A. Bennani, J.P. Bonnelle, A. Aboukaïs, J. Chem. Soc., Faraday Trans. 91 (1995) 99.
[14] R. Aasa, J. Chem. Phys. 52 (1970) 3919.
[15] A. Amorelli, J.C. Evans, C.C. Rowlands, T.A. Egerton, J. Chem. Soc., Faraday Trans. 83 (1987) 3541.
[16] A. Davidson, M. Che, J. Phys. Chem. 96 (1992) 9909.
[17] L.D. Bogomolova, A.N. Khabarova, E.V. Klimashina, N.A. Krasil’nikova, V.A. Jachkin, J. Non-Cryst. Solids 103 (1988) 319.
[18] F. Cavani, G. Centi, E. Foresti, F. Trifiro, G. Busca, J. Chem. Soc., Faraday Trans. 84 (1988) 237.
[19] T. Purcell, R.A. Weeks, J. Chem. Phys. 54 (1971) 2800.
[20] Y. Ono, K. Suzuki, T. Keii, J. Phys. Chem. 78 (1974) 218.
[21] T.T. Chang, Phys. Rev. 147 (1966) 264.